

https://dspace.org/

Digital data processing of marine seismic records from the South West Indian Ocean

Chetty, Parasuraman

2015-01-13
http://hdl.handle.net/10539/16504

Downloaded from a DSpace repository. https://dspace.org/

DIGITAL DATA PROCESSING OF MARINE SEISMIC RECORDS FROM THE S' WEST INDIAN OCEAN

by

PARASURAMAN CHETTY

A dissertation submitted to the Faculty of Engineering, University of the Witwatersrand, Johannesburg in partial fulfilment of the requirements for the Degree of Master of Science

April 1974

DECLARATION

I hereby declare that this dissertation is my own work and has not previously been incorporated in a dissertation for a degree at this or any other University.

PARASURAMAN CHETTY

CONTENTS

	Page
ABSTRACT	viii
I. INTRODUCTION	I
A. General	I
B. Experimental Techniques used at sea	I
C. Equipment at sea	2
D. Playback of magnetic tapes	3
E. Digital processing of records	4
F. Digital filtering	5
II. METHOD OF INTERPRETATION	7
A. Corrections	7
B. Water depth	7
C. Sediment structure	8
D. Velocity determination	9
E. Depth sections	11
III. SEISMIC STUDIES ON THE CONTINENTAL SHELF AND SLOPE	12
A. Profile 20	12
B. Profile 14	13
C. Geological setting	14
D. Velocity correlation with geology	16
IV. SEISMIC STUDIES IN THE TRANSKEI BASIN	18
A. Profiles 15 and 17	18
B. Discussion of the Transkei basin profiles	20

		Page
V.	SEISMIC STUDIES ON THE MOZAMBIQUE RIDGE	23
A.	Profile 16	23
B.	The Preferred Interpretation of the Mozambique Ridge	24
C.	Can the Mozambique Ridge data be interpreted as continental crust?	25
VI.	GENERAL CONCLUSIONS ABOUT THE SOUTH WEST INDIAN OCEAN	27
	A C K N O W L E D G E M E N T S	31
	R E F E R E N C E S	32

I L L U S T R A T I O N S

Figures		Facing Page
1	Map of the survey area showing the locations of the profiles	1
2	Schematic diagram of ship equipment	2
3	Schematic diagram of buoy equipment	3
4	A typical hard copy record from the Transkei Basin	4
5	Schematic diagram of tape playback system	4
6	Shape of digital filter used in filtering the digital Record Sections for different values of 'X'	5
7	Frequency spectra of the first refracted arrival from a 160 kg depth charge and a 14 kg shot	6
8	Observed and theoretical travel times (profile 15, buoy 2) For R_2, R_1R_2 and R_2R_2 for different velocity gradients	8

Figures		Facing Page
9	Travel-time plot for profile 20	12
10-11	Record Sections from buoys 2 and 3, profile 20	12
12	Travel-time plot for profile 14	13
13-14	Record sections from buoys 1 and 3, profile 14	13
15-18	Reflection record sections from buoy 1, profile 15 and buoy 2, profile 17	18
19-20	Travel-time plots for profiles 15 and 17	19
21-23	Refraction Record Sections from buoys 1 and 3, profile 15 and buoy 3, profile 17	19
24	A summary of the results of seismic profiles in the Transkei Basin. Profile G18 is from Green and Hales (1966) and profiles H(11-13) from Hales and Nation (1973)	20
25	Reflection Record Section from buoy 2, profile 16	23
26	Travel-time plot for profile 16	24

Figures		Facing Page
27-28	Refraction Record Sections from buoys 1 and 3, profile 16	24
29	A summary of the results of seismic profiles on the Mozambique Ridge. Profiles H(14-16) from Hales and Nation (1973)	25
30	Histograms of distribution of velocities and mantle depths for the S.W. Indian Ocean, N.W. Indian Ocean, S. Indian Ocean, the entire Indian Ocean and the Pacific Ocean	27

TABLES

Table		Facing Page
1	Apparent velocities, intercept times, true velocities, thicknesses and dips from buoys 2 and 3, profile 20	12
2	Apparent velocities, intercept times, true velocities, thicknesses and dips from buoys 1 and 3, profile 14	13
3	Locations of stations, velocities and thicknesses for profiles 20, 152 (Ludwig et al, 1968) and 14	16
4	Velocities, thicknesses and probable formation of layers on the continental shelf and slope	17
5	Root mean square deviations for travel times of model structures and observations for profiles 15 and 17	18
6	Water and sediment structure for profiles 15 and 17	18
7	Apparent velocities and intercept times for profiles 15 and 17	19

Table		Facing Page
8	True velocities, thicknesses and dips for profiles 15 and 17	19
9	Root mean square deviations for travel times of model structures and observations for profile 16	23
10	Water and sediment structure for profile 16	23
11	True velocities and thicknesses for profile 16 and profile 14 of Hales and Nation	24

Abstract

This dissertation describes the interpretation of five seismic refraction profiles on the continental shelf and slope, the Transkei Basin and the Mozambique Ridge of the South Western Indian Ocean. Velocities from 1.98 to 3.51 km/sec obtained for the continental shelf, and slope profiles are correlated with sediments of Cretaceous and younger age. Directly below this group are rocks with velocities in the range 4.0 - 5.5 km/sec, probably representatives of the Karroo and Cape Supergroups. The basement is comprised of rocks with velocities 6.31 and 5.94 km/sec which is consistent with granite at this depth of burial.

The profiles in the Transkei Basin show a thick layer of sediment with velocity range 1.51 to 3.57 km/sec, underlain by a refracting layer in which the average velocity is 4.5 km/sec. The velocity of 6.6 km/sec obtained for the oceanic layer is similar to the velocities of the crustal layer measured in the Argentine Basin and the Pacific Ocean. The mantle velocity 8.1 km/sec is consistent with the average mantle velocity for the Indian Ocean but significantly lower than the Pacific Ocean average of 8.20 km/sec. A plate tectonic model of the early opening of the South Atlantic is used to describe the evolution of the Transkei Basin.

On the Mozambique Ridge the thin sediments (0.7 km) are underlain by two refracting layers with velocities averaging 2.27 and 5.65 km/sec. The profile was not long enough to determine velocities from layers deeper than the 5.65 km/sec material. This seismic velocity structure of the upper portion of the profiles on the ridge is very similar to the upper section of several profiles off the East African Coast as reported by Francis et al, and Francis and Shor. The crustal section of the Ridge was determined by Hales and Nation (22 km to the Moho discontinuity); they also report that the Ridge is in isostatic equilibrium when compared

with the adjacent Transkei Basin. The preferred interpretation of the Mozambique Ridge is that of an oceanic crust; however, interpretation in terms of a subsided continental fragment cannot be categorically excluded.

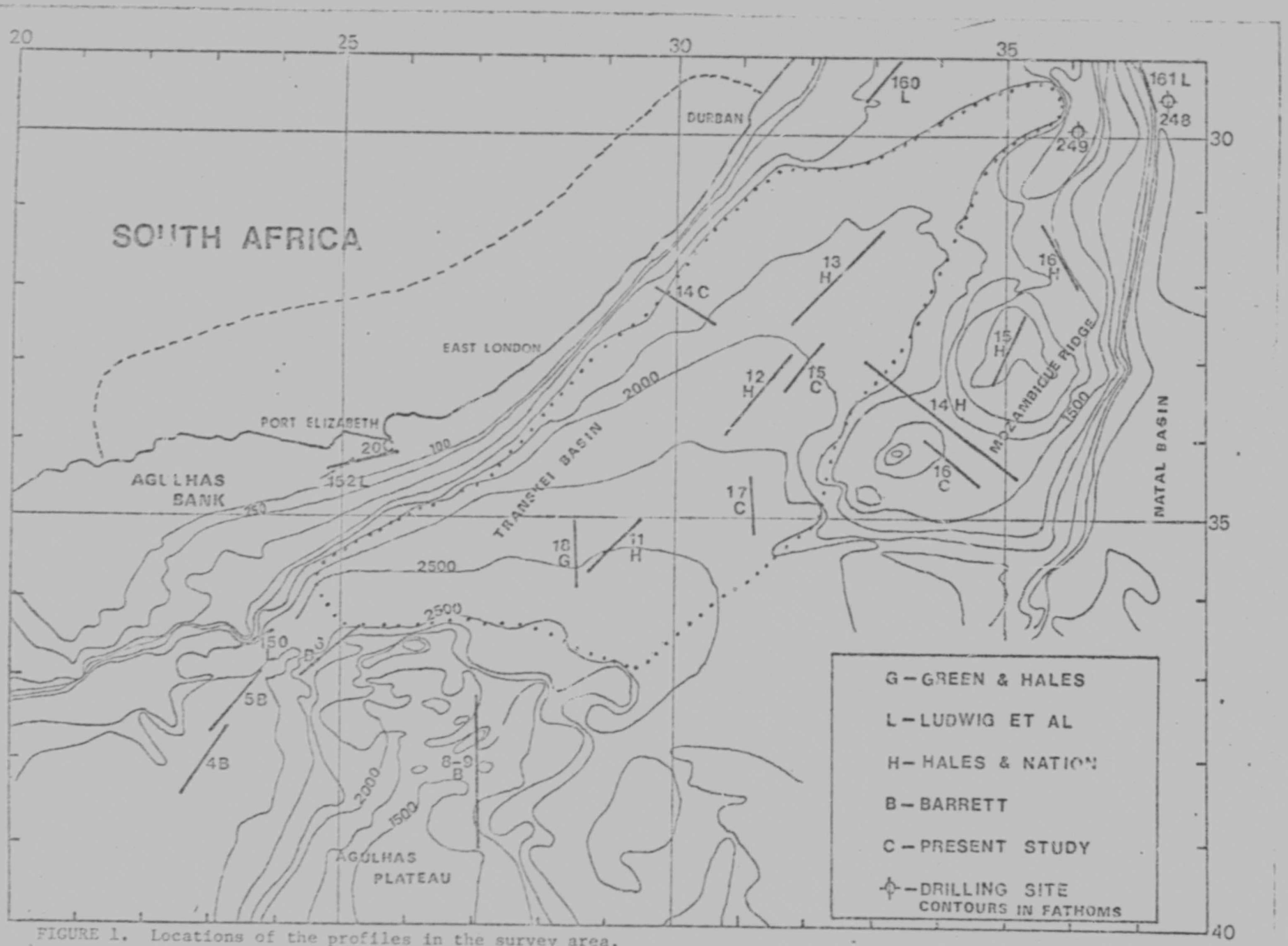

FIGURE 1. Locations of the profiles in the survey area.

DIGITAL DATA PROCESSING OF MARINE SEISMIC RECORDS FROM THE SOUTH WEST INDIAN OCEAN

I. Introduction

A. General

As part of South Africa's participation in the International Indian Ocean Expedition (IIOE), seismic refraction investigations were carried out in portions of the South Western Indian Ocean during May and June of 1962. The results of two of the profiles have been reported (Green and Hales, 1966) but five profiles remained to be interpreted. I have recently undertaken this interpretive work under Green's supervision, and the results are reported in this study.

The profile regions include the continental shelf area of the Pondoland coast, the Mozambique Ridge and sites in the adjacent Transkei basin. Figure (1) shows the locations of the profiles together with all the refraction lines reported for these areas. These include the profiles of Green and Hales (1966), Ludwig et al (1968), Hales and Nation (1973) and Barrett (private communication).

B. Experimental Techniques used at Sea

A single ship technique was developed for the seismic refraction studies (Green and Hales, 1966). The three recording buoys which acted as receiving stations were normally spaced 10 km apart, and this ensured that the profile would be effectively overlapped by at least two of the buoys. The first 160 kg depth charge shot was dropped 60 km distant along the line of buoys on the one side and the last shot at the corresponding distance on the other side. Close to the buoys 5, 11 and 23 kg of

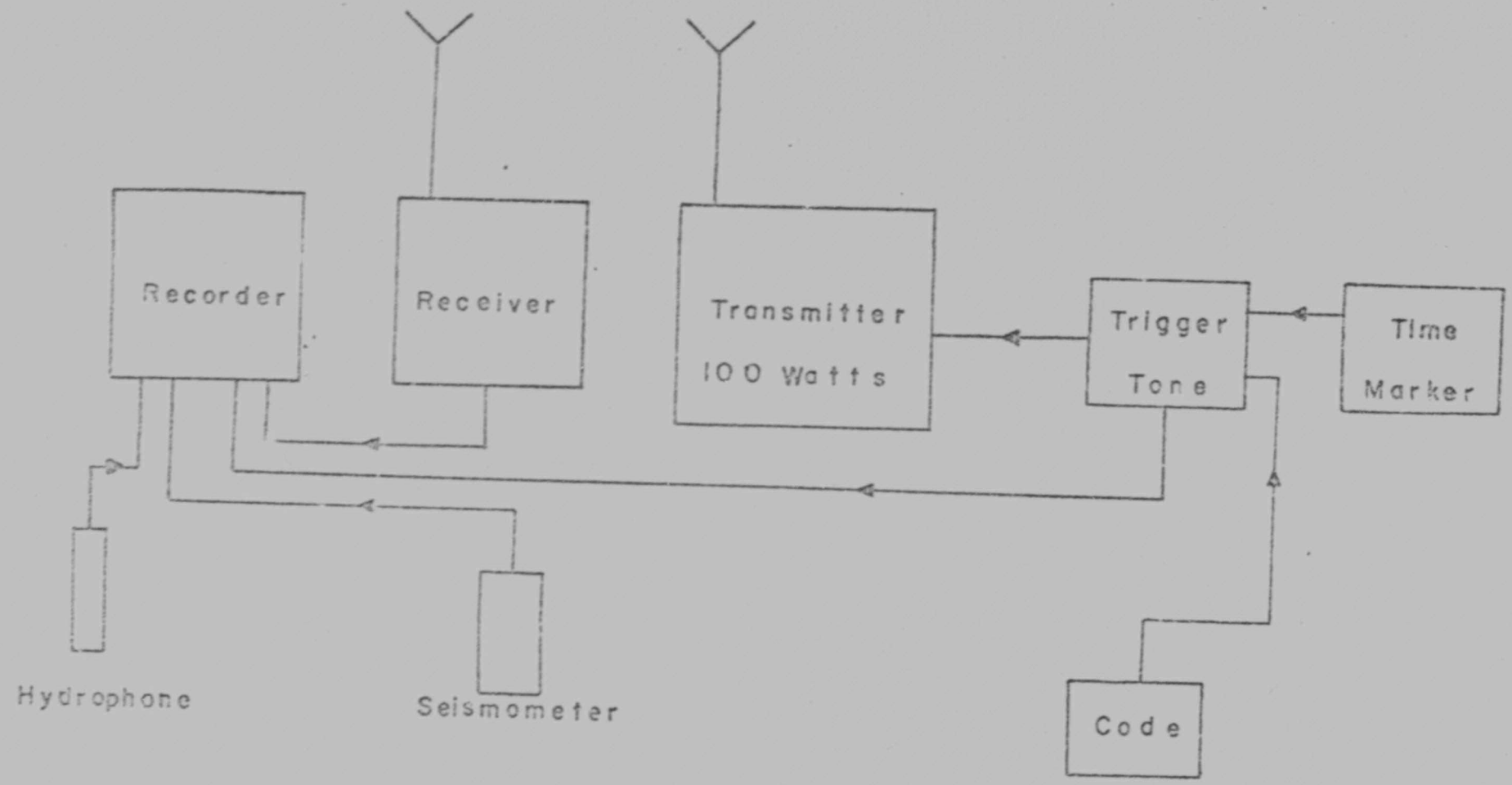

FIGURE 2. SCHEMATIC DIAGRAM OF SHIP EQUIPMENT.

explosives (geophex) were fired using burning fuse delays. The ship cruised at 10 to 12 knots so that from the time of dropping the buoys until recovery about eleven hours elapsed.

C. Equipment at Sea

The ship's equipment is shown in block form in figure (2). Portable tape recorders with the required time resolution, weight and power consumption combined with an endurance of eleven hours were not available, and accordingly it was decided to use a triggered tape recording system. The trigger tone was provided by a 1000 Hz tuning fork which modulated a 7.9 mc/s transmitter. The modulation was suppressed for one-tenth of a second every half second, and these breaks were used as time marks. The time marks were coded so that the time marks on buoy records could be correlated with the shot instant records obtained on the ship. The shot time was obtained from a towed hydrophone and a back up seismometer on the ship and recording was carried out on a 35 mm photographic reading paper camera running at about 4 cm/sec.

The equipment that made up the buoy package is shown in block form in figure (3). The 7.9 mc/s receiver was designed for the unattended stations of an earth tremor program. The demodulated signal from the receiver was channeled to a tuning fork filter unit and the filters rectified output was used as the trigger bias to start the tape transport. The triggering time was about 2 seconds and the unit had a built in 'hold on' of about 12 seconds to cope with radio fading. The unfiltered receiver signal was recorded on one of the tracks of the twin track tape recorder and this provided the time trace.

The tape recorder was a standard portable operating on internal batteries. It had been modified by replacing the single track head with a twin track system and the 'on' switch was relay activated by the output

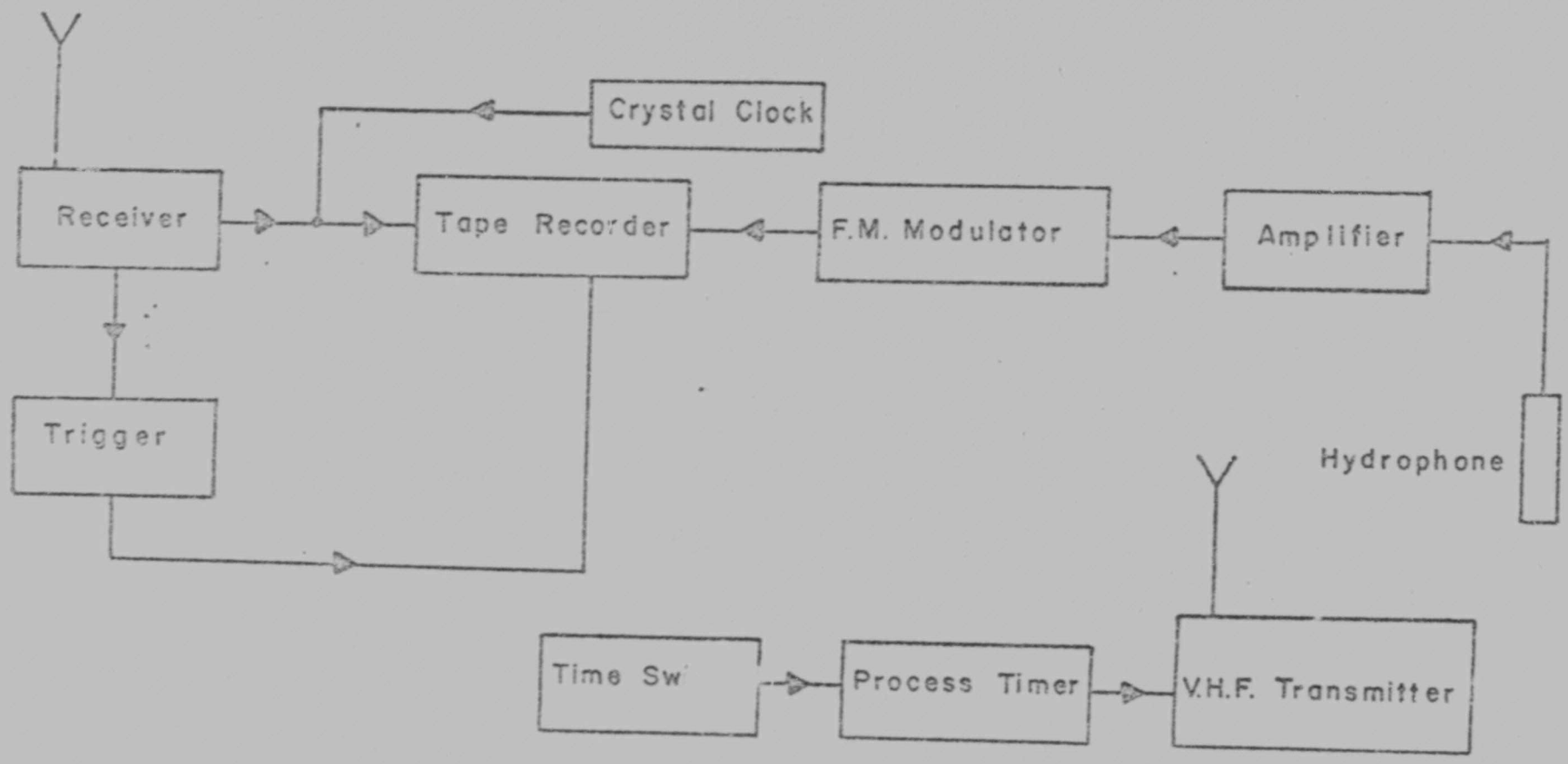

FIGURE 3. SCHEMATIC DIAGRAM OF BUOY EQUIPMENT.

of the tuning fork filter unit. The hydrophones that were used were E V P 5's and these were suspended at a depth of about 52 meters. The hydrophone signal was amplified by a wide band (4-600 Hz) amplifier and then recorded as an F.M tone that utilized a center frequency of 5 kHz. The tape was 12.7 mil 6.4mm wide tape and the recorder had a total recording time of 35 minutes.

For the first profiles the buoy equipment included a V.H.F. transmitter and a crystal clock. The clock was included since it had been found in the land work that the trigger unit would work when the 1000 Hz signal was completely masked by noise and no time marks could be recorded, at sea however, the time marks were always good and the clock was not used for the later profiles. The V.H.F. transmitter was controlled by a time switch so that it transmitted for five minutes every half hour beginning at a preset time from 8-12 hours after the buoys were dropped. It was intended that this signal should serve for the location of the buoys. The other locating device was a 90 cm diameter hydrogen filled meteorological balloon tethered to the buoy on a 60 meter line. As a result of excellent navigation on the S.A. Natal and the good visibility of the balloon the V.H.F. transmitter location system proved to be unnecessary and it was not used on the later profiles.

D. Playback of Magnetic Tapes

Prior to use of the Institute's facility for the digitising and computer handling of geophysical data, the records were replayed via a standard recorder into a multichannel recording oscillograph. After demodulation the signal was passed through a set of filter units, the cut off frequency set for 600 to 150 Hz, 150 to 50 Hz, and 4 to 50 Hz, the roll off being 18db/octave. One trace was left unfiltered in order to verify that relevant information was not lost or added in the filtering

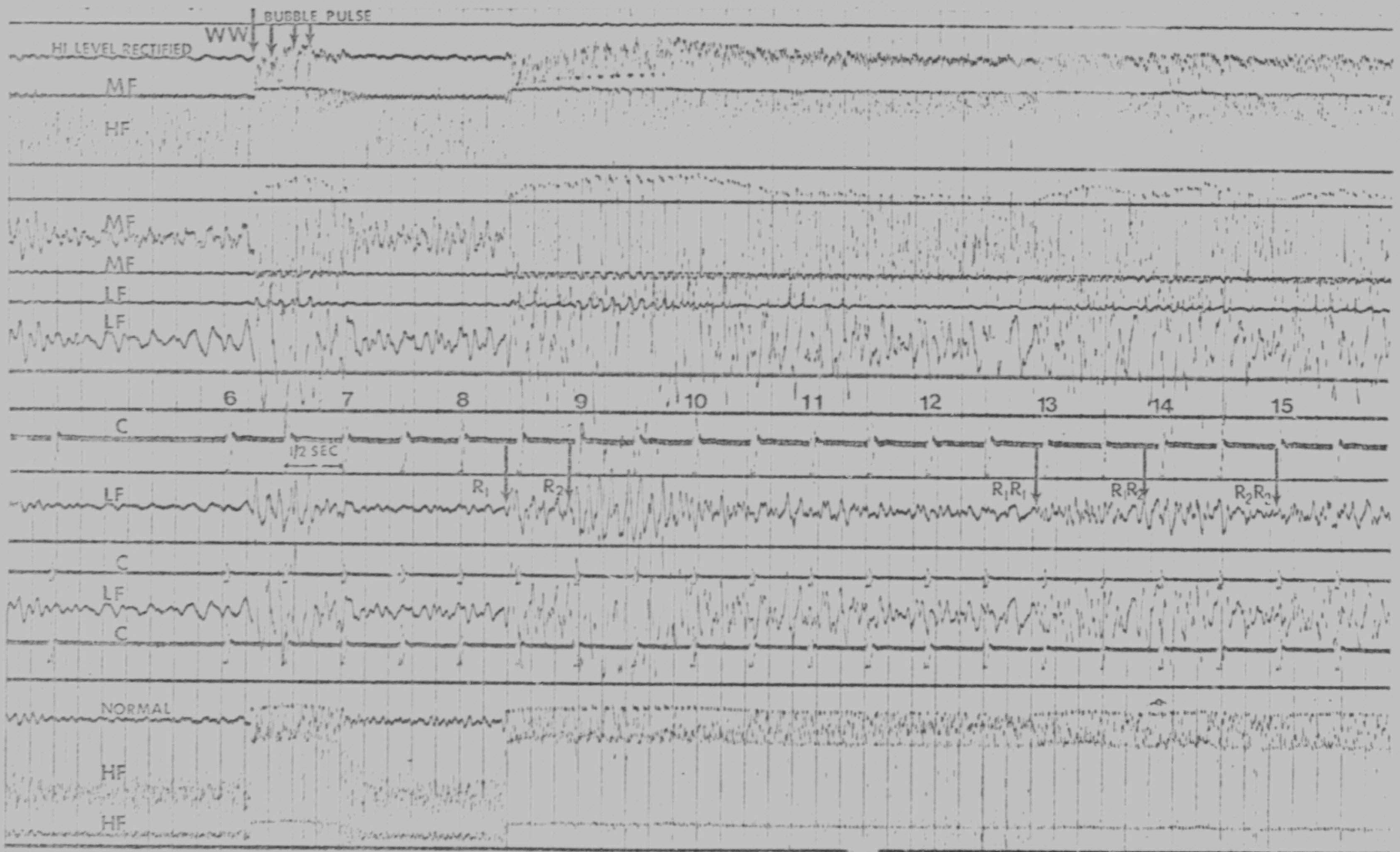

FIGURE 4. A TYPICAL HARD COPY RECORD

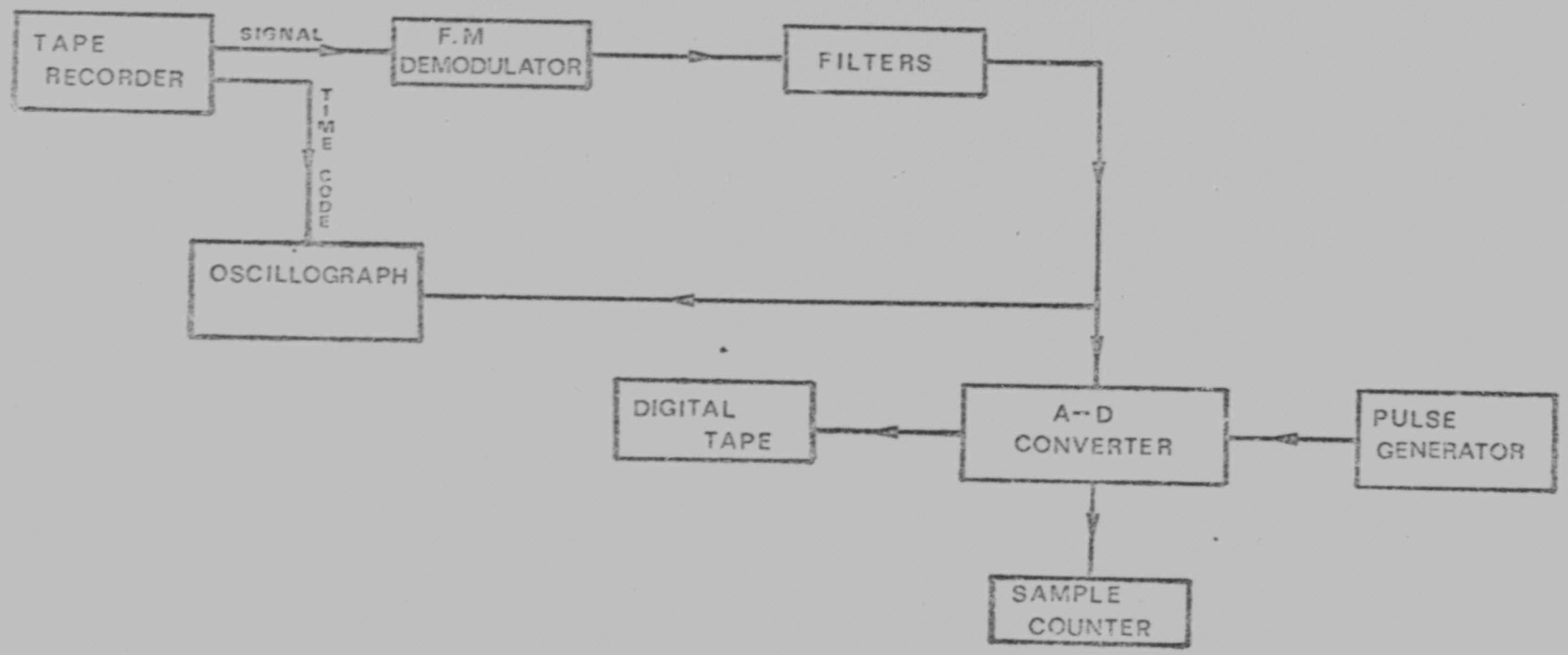

FIGURE 5. SCHEMATIC DIAGRAM OF TAPE PLAYBACK SYSTEM

process. The high pass channel was used to pick the time of arrival of the direct wave through the water whilst reflections and refractions were normally obtained from the low frequency channels.

Figure (4) shows a typical 'hard copy' record from the Transkei basin, as obtained with the original replay equipment. WW is the direct arrival through the water. The bubble pulse shows clearly. The first reflection from the ocean bottom is followed by the sub-bottom reflection; these are marked R_1 and R_2. The multiple reflected arrivals are R_1R_2 and R_2R_2 with the subscripts refering to the reflecting layer. Channels marked C are the clock traces with 1/2 sec time marks.

After the construction of the institute's anologue-digital converter (Green 1973) the tapes were digitised and record sections were generated to aid in the interpretation of the data and figure (5) is a block diagram of the equipment utilized in this process.

The tape recorder used for the replay was similar to the one used in the original buoy equipment and playback speed was 952.5 mm/sec. After demodulation the signal was passed through a filter unit set with a bandpass of 3 to 170 Hz. The pulse generator was adjusted so that a digitising rate of 500 samples/sec was obtained. The length of time that a record had to be digitised was set up on the tape search and control unit and together with the time code translator which was pulsed by the pulsegenerator, control of the digitised tape could be obtained in terms of the pulse rate. The number of samples taken during that time interval was recorded on the sample counter. The digital transport generates a standard 9 track I.B.M. format tape with 360 compatibility

E. Digital Processing of Records

To prevent aliasing the digitisation rate was always more than 340 samples/sec as the Nyquist frequency was 170 Hz.

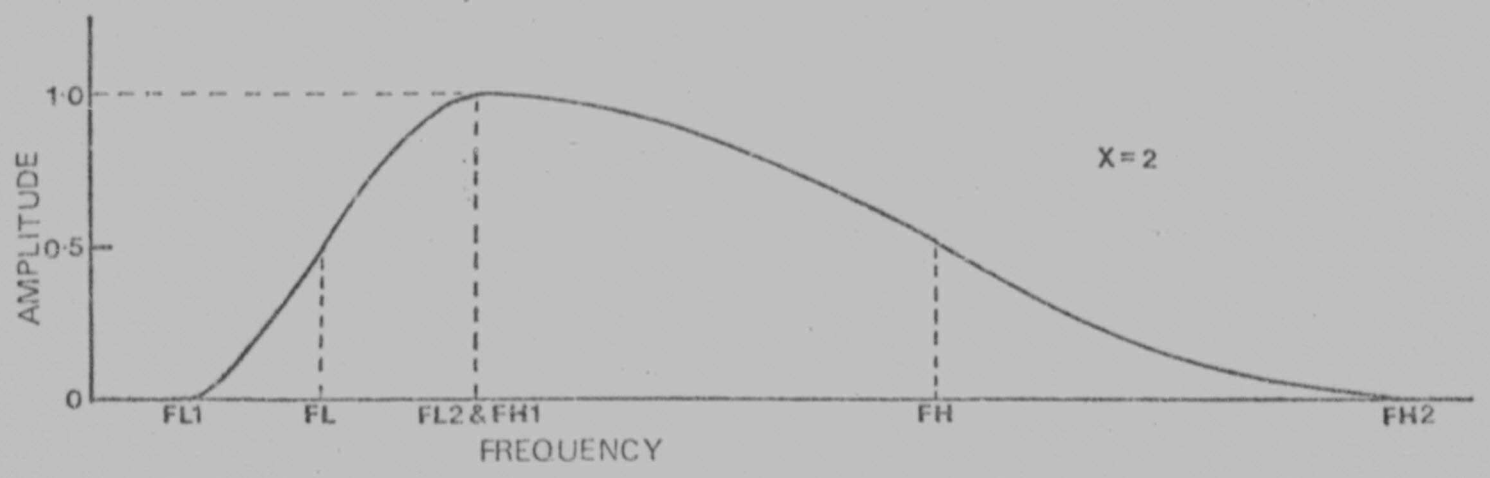

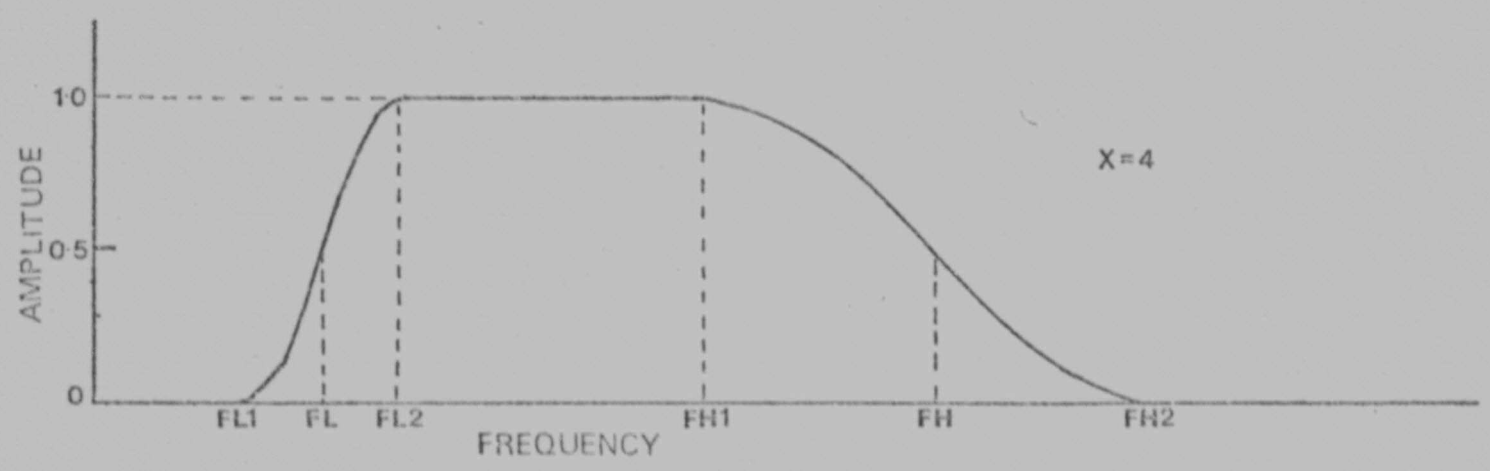

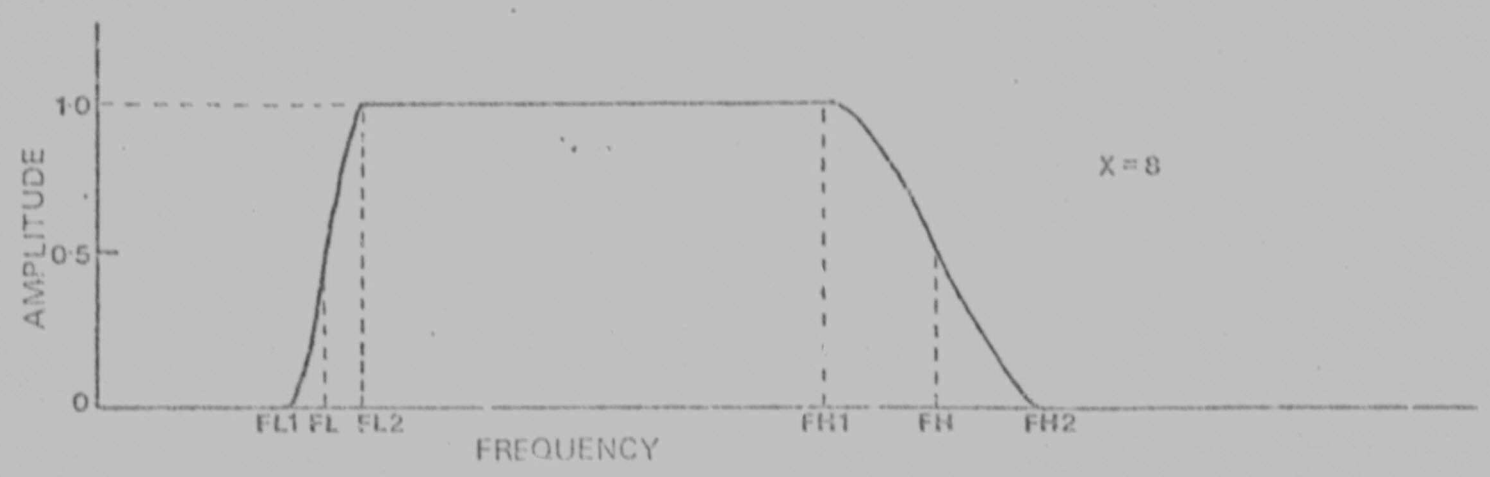

FIGURE 6. Shape of digital filter used in filtering the digital record sections for different values of 'X'.

The program used to read the digital tapes and to produce record sections on the plotter, required the following information for each shot; (i) distances from the buoy (ii) digitisation rate (iii) amplitude and (iv) the band pass filter points. These data was obtained from the hard copy records.

Due to the variations of speed of the tape recorder and the oscillograph the effective sampling rate varied from 400 to 500 samples/sec. This variation had to be considered when the computer record sections were plotted and the individual records had to be corrected so that the time of a particular arrival corresponds to the same time on the oscillograph records. This procedure did not however correct the travel times of the later arrivals.

F. Digital Filtering

Digital filtering techniques were applied to the record sections to enhance the seismic signal in the presence of noise. In order to design a suitable filter a knowledge of the characteristics of both the signal and the noise is needed.

Digital filtering can be performed by multiplication in the frequency domain or by convolution in the time domain.

$$F(W).\ G(W) \longleftrightarrow \int g(x).f(t-x)\ dx$$

where f(t) is the time series to be filtered and g(x) is the Fourier transform of G(W). The desired filter function g(x) must be symmetric in order that the filter not alter the phase function f(t).

The filtering in this study was done in the frequency domain using the I.B.M. scientific subroutines Rharl and Harm. The shape of the digital filter used is given in figure (6). The filter is cosine tapered and is symmetrical. The filter was tapered so as to prevent ringing. Its coefficients are given by

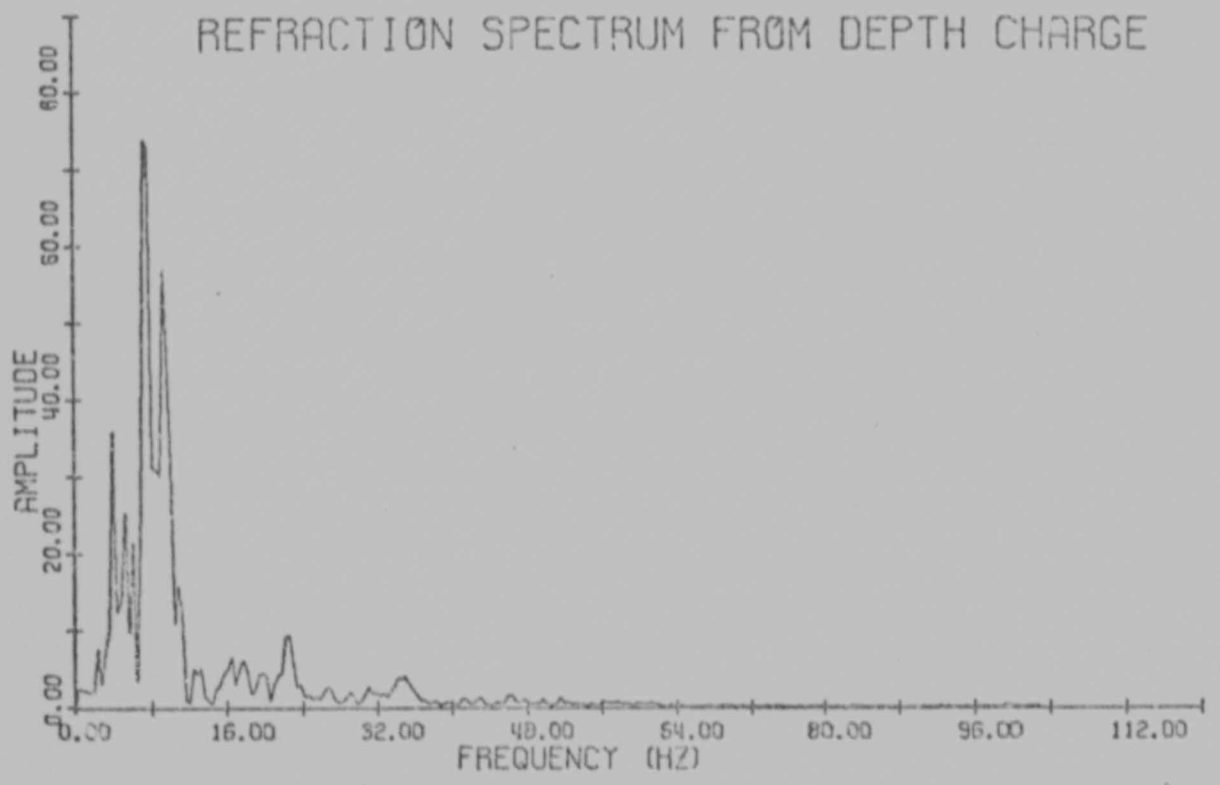

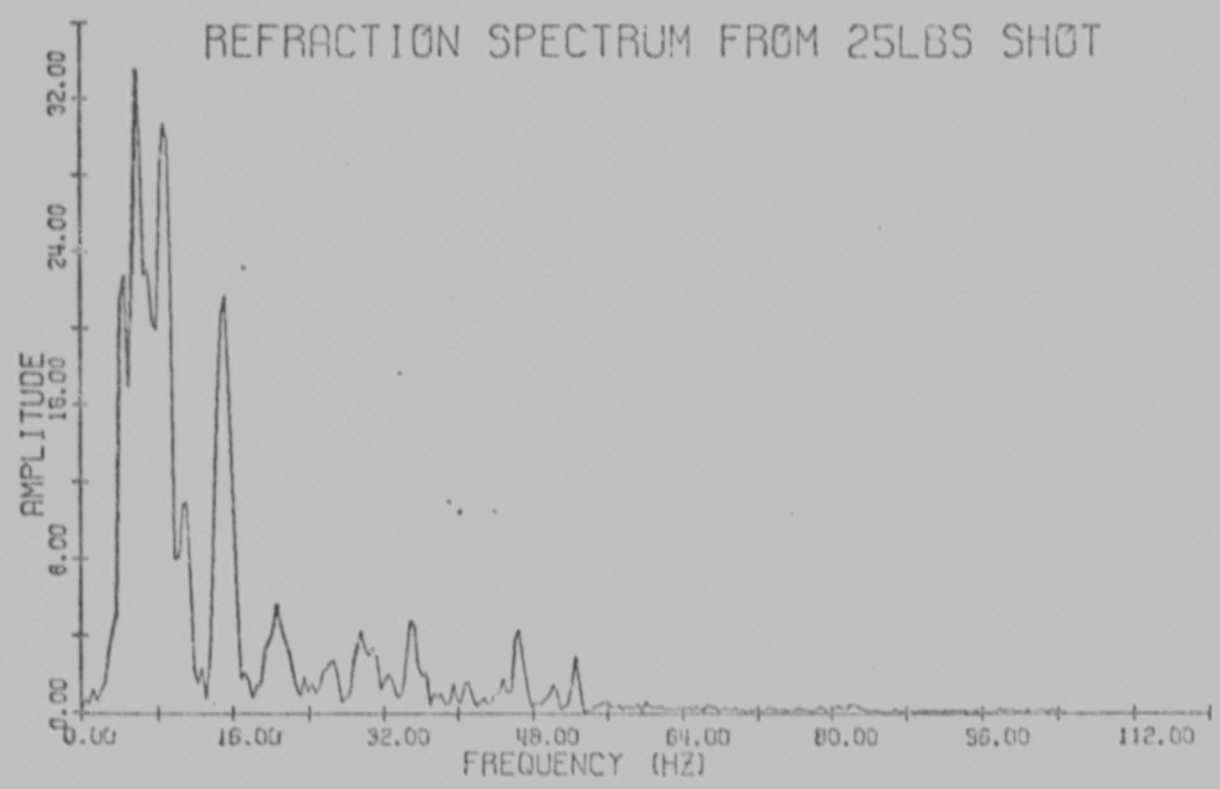

FIGURE 7. Frequency spectra of the first refracted arrival from a 160 kg depth charge and a 11 kg shot.

$$FL1 = FL - FL/X$$

$$FL2 = FL + FL/X$$

$$FH1 = FH - FH/X$$

$$FH2 = FH + FH/X$$

where FL and FH are the band pass frequencies. Several values for 'X' were tested and the optimum value was 4.0. This gave a roll-off of 12 db/octave. Higher values than 4.0 caused ringing and the values lower than 4.0 slurred out the cosine function and passed more of the lower and higher frequencies.

To improve the signal to noise ratio of the refracted arrivals the records were filtered using the above filter with center frequencies 5 and 20 Hz. Figure (7) gives the frequency spectra of the refracted arrivals from a depth charge and a 11 kg shot. As can be seen maximum energy is concentrated in the range 4 to 20 Hz.

II. Method of Interpretation

A. Corrections

The sinking rate for the 5, 11 and 23 kg shots were determined experimentally by dropping respective weights attached to a rope over the side of the ship and measuring the distance travelled in a given period of time. The sinking rate was approximately 1.4 m/sec. This value was confirmed from measurements of the time difference between the first and second bottom reflections. The sinking rate 2.55 m/sec for the depth charge was taken from the curves published by Officer and Vuenschel (1951). Knowing the time arrival of the direct wave through the water, the time the explosive went over the side of the ship, the speed of the ship and the depth to which the shot sank, the shot instant time and surface corrections can be calculated.

B. Water Depth

To determine the water depths for the profiles where refractions from the top of the sediment were absent reflections (R_1) were used for each buoy of the profile. These high frequency arrivals are strong and were clearly visible on the reflection record sections. It can be shown that for R_1

$$T^2 = (X^2 + 4H_o^2)/V_o^2$$

where T, H_o, V_o and X are the travel time, thickness, average velocity in the water and shot distance respectively. The shot distance was obtained by reading the time of arrival of the direct wave through the water and multiplying by the average horizontal water velocity. A mean velocity of 1.51 km/sec was used for the water throughout the calculations. A least squares solution of the parameters T^2 and X^2 yielded the water depth H_o. An arithmetic average of the water depth was used for profiles where

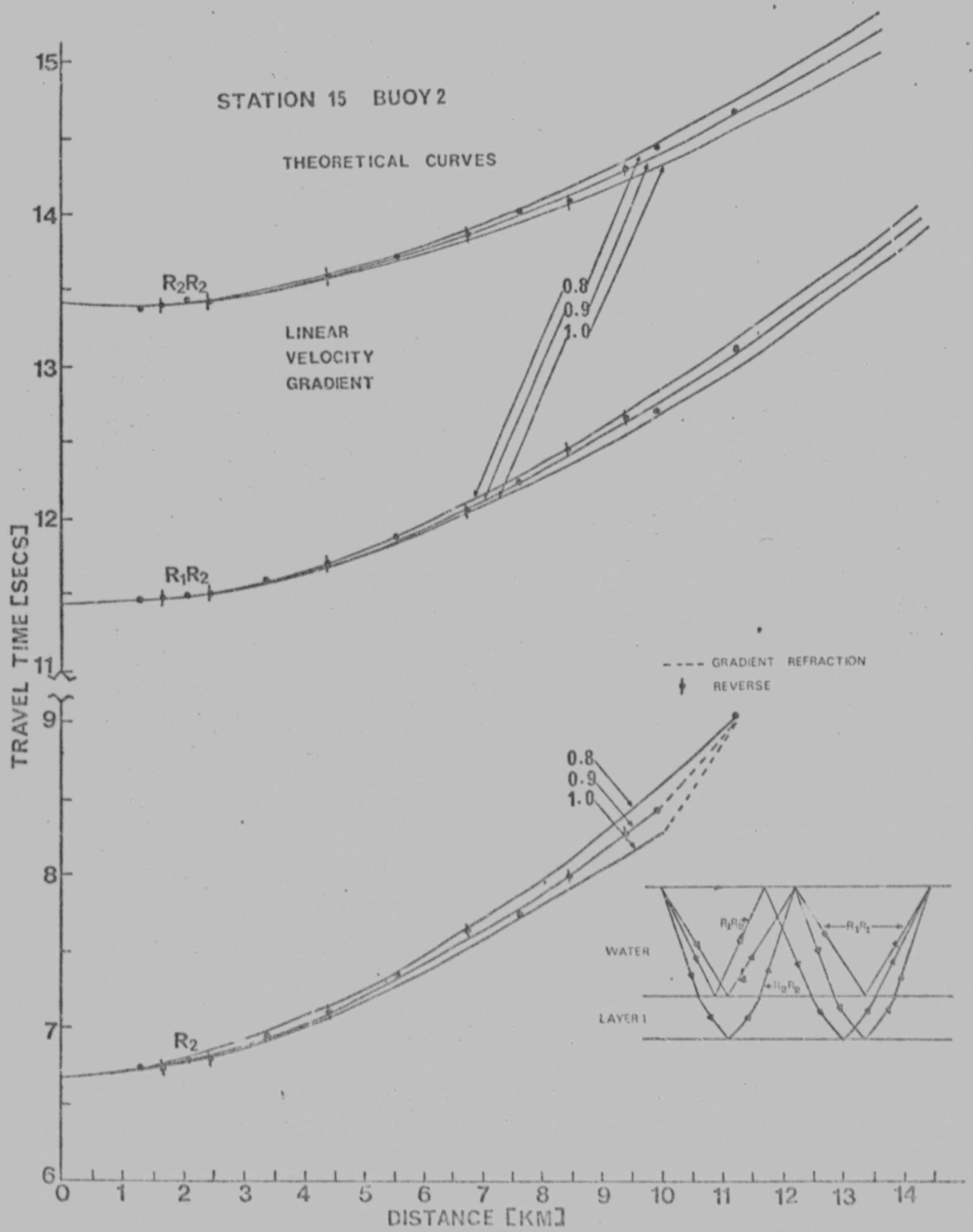

FIGURE 8. Observed and theoretical travel times (profile 15, buoy 2) for R_2, R_1R_2 and R_2R_2 for different velocity gradients.

more than one buoy worked. Shots closer than 15 km to the buoy were used for reflection data as it was found that the difference between actual water depth and the depth computed for the point of reflection increased with increasing distance. This effect is due to the velocity gradient in the water.

C. Sediment Structure

The sediment structure for profiles 15, 16 and 17 was obtained by fitting models to the reflected arrivals R_2 and the multiple arrivals R_1R_2 and R_2R2. The ray paths for these arrivals are shown in figure (8). These arrivals are outstanding features on all the buoy records, with the energy associated with them increasing from R_1R_1 through to R_1R_2 and R_2R_2 at distances greater than 12 kms. This energy increase can be attributed in part to a very low reflection coefficient between the water sediment interface and a relatively high reflection coefficient between the unconsolidated material and the sub-bottom reflector as suggested by Green and Hales (1966).

To determine the velocity gradient in the unconsolidated sediments theoretical travel time curves were computed for R_2, R_1R_2 and R_2R_2 for model structures and these were then compared with the observations. Using the average water depth calculated from the bottom reflections R_1 and assuming horizontal layering two models were investigated:

(i) The sedimentary velocity increases linearly with depth of burial and

(ii) the velocity increases at a rate proportional to the square root of the depth of burial.

A program was run to compute the travel times for R_2, R_1R2 and R_2R_2.

It can be shown that for case (i) above the time spent in the sediment is given by

$$T = (1/g)\log\left\{V\left[1+(1-P^2V_o^2)^{\frac{1}{2}}\right] \Big/ \left[1+(1-P^2V^2)^{\frac{1}{2}}\right]V_o\right\}$$

where $V = V_o + gh$

and for case (ii)

$$T = (2/Pg^2)\left\{\arcsin PV - \arcsin PV_o + PV_o \log\left[V_o(1+(1-P^2V^2)^{\frac{1}{2}})\Big/ V(1+(1-P^2V_o^2)^{\frac{1}{2}})\right]\right\}$$

where $V = V_o + gh^{\frac{1}{2}}$

$P = \sin a/V_o$ $\quad$ a = angle of incidence

V_o = velocity at the top of the sediment

g = velocity gradient

and h = depth of burial (Slotnick,1959)

All the calculations were carried out using a velocity of 1.51 km/sec at the top of the sediment. The theoretical curves for case (i) and the observations for profile 15, buoy 2 are shown in figure (8). The velocity corresponding to each observation was estimated by interpolating between the curves. A least square method was used to calculate the standard deviation for the different models run. The model with the minimum standard deviation was taken as the best fit to the observations. Case (ii) was run for profile 15 and it gave a poorer fit than case (i). For all the profiles a linear velocity gradient of 0.9 sec^{-1} was found to fit the data best.

D. Velocity Determination

After reading the hard copy records, the data for each buoy were plotted as travel time curves. These travel time curves were partitioned into straight line segments, corresponding to refractions from various layers. Using Ewing's method (Ewing et al, 1940) of least squares for overlapping profiles a computer program was run to compute the intercept time and apparent velocities in both directions. The method has the advantage that a single data point from a buoy can be made use of in the

interpretation since it combines all the data from all the buoys of a single profile. The formulae are based on the following assumptions and relations;

(i) Each layer is bounded top and bottom by planes and transmit seismic waves at a constant velocity.

(ii) At the interface between two layers the path of the seismic wave is bent according to Snell's law $\sin a_1/\sin a_2 = V_1/V_2$ where a_1 and a_2 are the angles of incidence and refraction and V_1, V_2 the velocities in the respective layers.

(iii) A wave travelling in any layer with velocity V and incident upon the surface of a layer at an angle a with the normal has on apparent velocity V/sina along the surface.

(iv) Any travel time will be unchanged if shot point and recording point are interchanged.

(v) The 'reverse points' of any oppositely directed overlapping pair of profiles must be equal.

(vi) The 'time intercept' points for each layer for all profiles of the group must be collinear

In cases where the actual condition deviates lightly from the assumptions-where for instance an interface is not perfectly plane-the solution gives the plane which best approximates the actual surface.

The travel time plots together with the record sections for the five profiles are given in the following chapter (iii). The equations for each straight line segment of these plots were determined by the above method and the apparent velocity and intercept time obtained is

noted adjacent to the line. For clarity solid lines were drawn joining the refractions from various layers on the record sections, these lines do not signify that a arrival from a layer was utilised from all the records. The arrival utilized from the records are given in the travel time plots.

E. Depth Sections

For computing the true velocity, dip and thickness of each layer the stepwise process of Ewing (1963) was employed. An average velocity for the unconsolidated sediment was used for profiles 15, 16 and 17. The intercept time for the layer immediately below the sediment is given by;

$$T = 2H_0(V_2^2 - V_0^2)^{\frac{1}{2}}/V_0V_2 + 2H_1(V_2^2 - V_1^2)^{\frac{1}{2}}/V_1V_2$$

for horizontal layering. Ho and Vo are the water thickness and velocity. H_1 the sediment thickness calculated from reflection data and V_2 the velocity for the layer below the sediment that was obtained from refraction data. Thus the equation maybe solved for V_1, the average velocity of the sediment. Where the difference in the apparent velocities from a layer were insignificant the arithmetic average of the two velocities were used.

Estimates of errors in the apparent velocities were calculated using the formula of Dowling (1968). He has also shown (1970) that velocity uncertainties do not propagate very strongly in seismic refraction calculations and that the uncertainties in the overlying layers can be neglected. The errors given are the standard deviations in the apparent velocities.

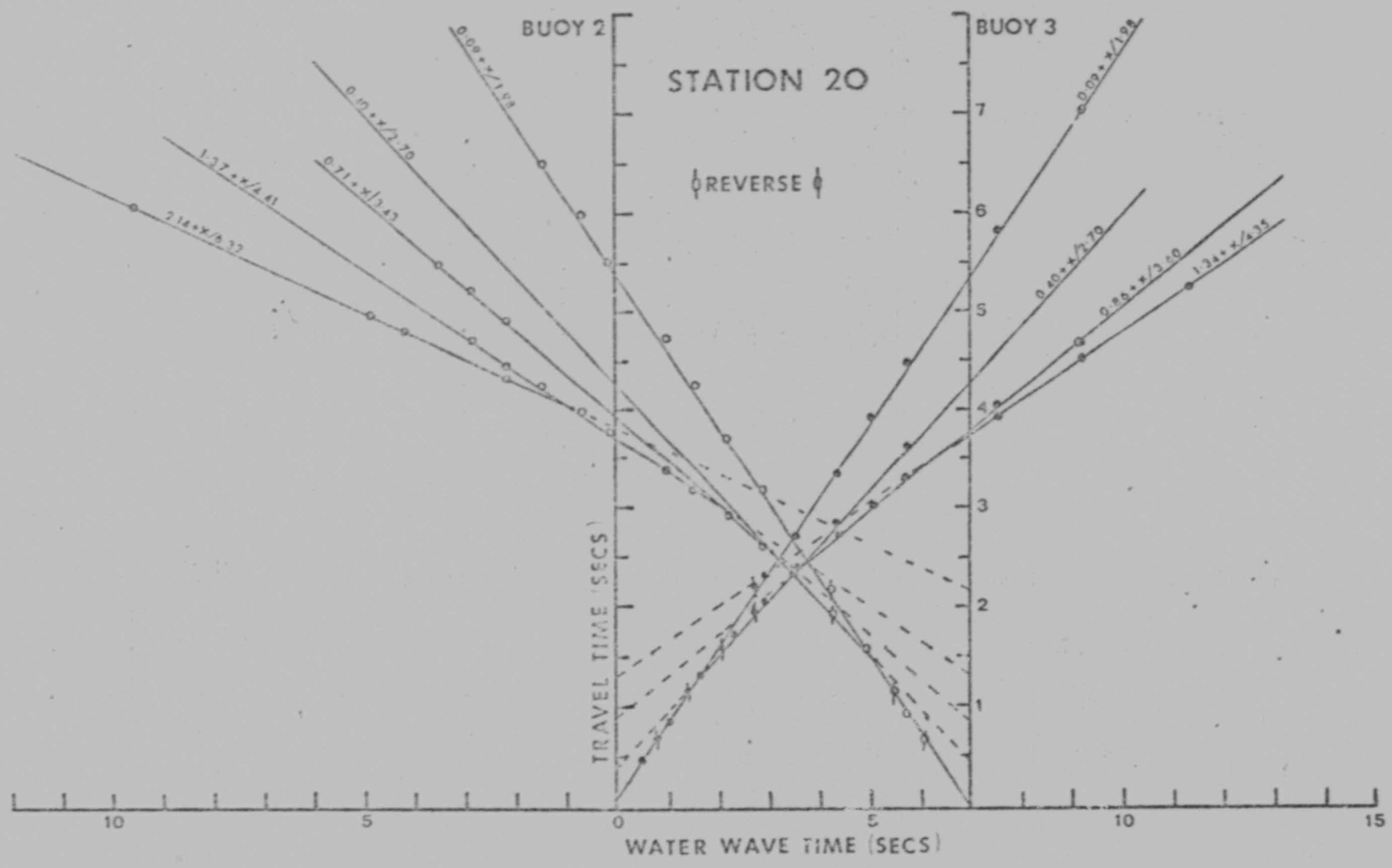

FIGURE 9. Travel-time plot for profile 20.

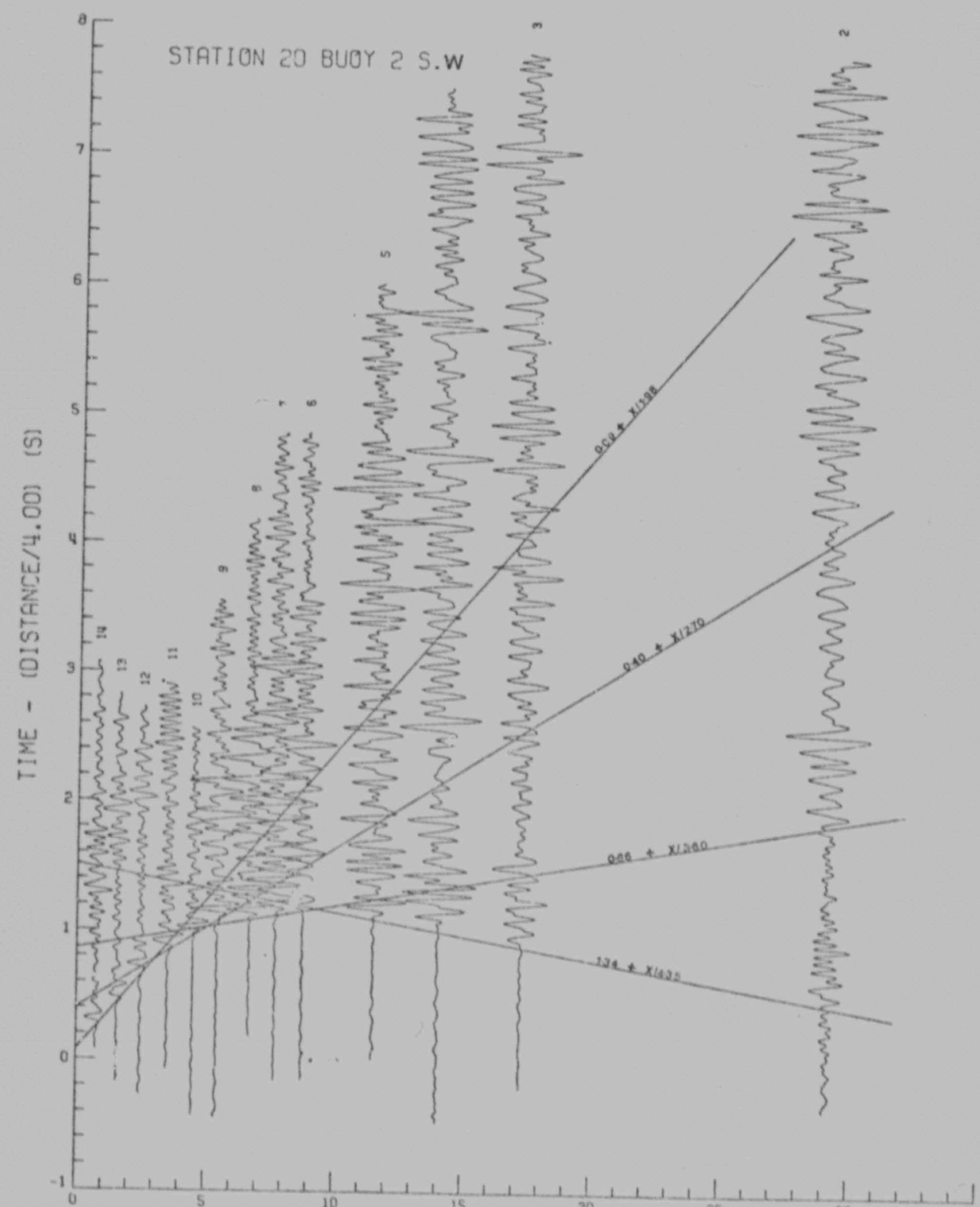

FIGURE 10. Record section from buoy 2, profile 20.

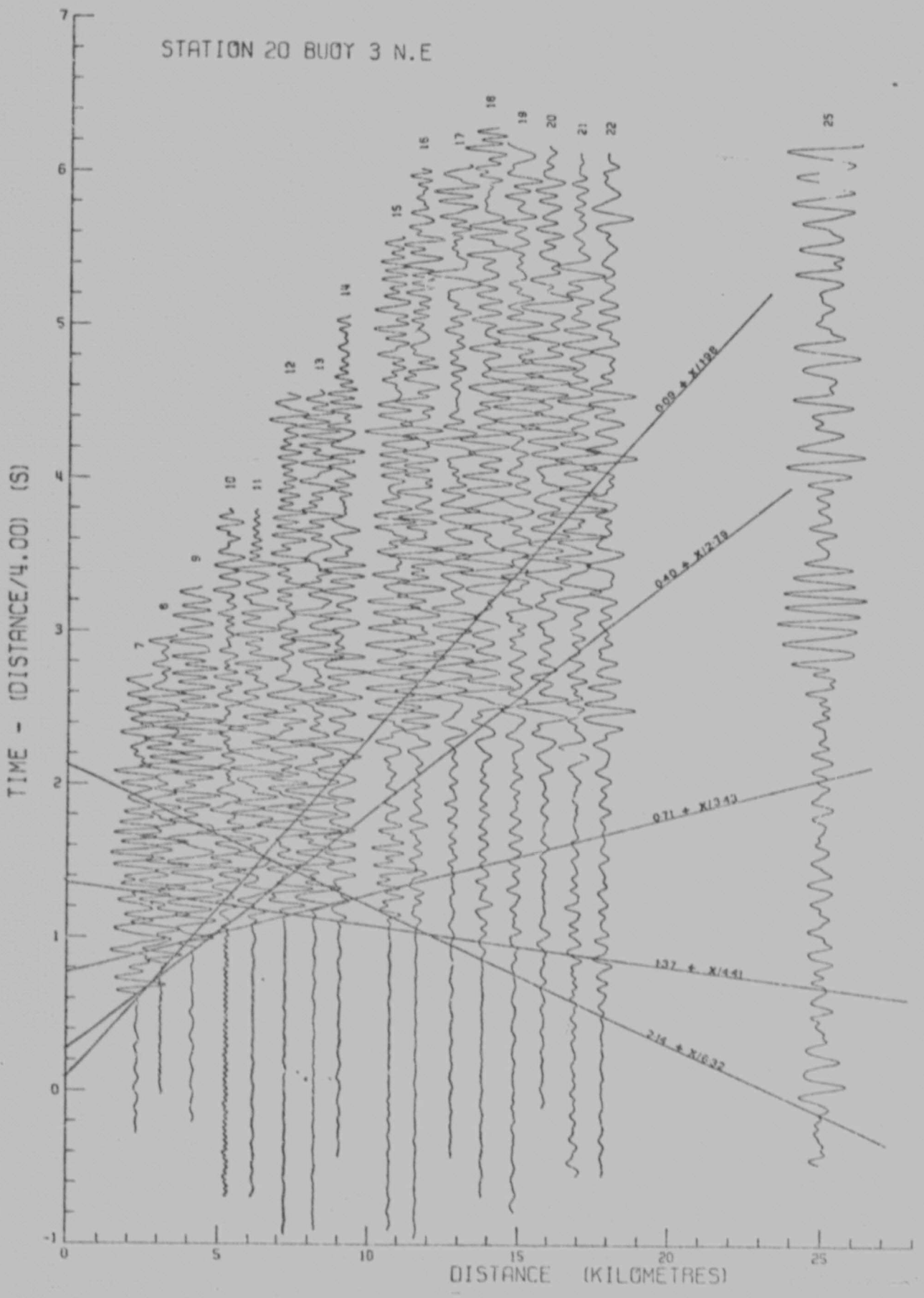

FIGURE 11. Record section from buoy 3, profile 20.

Table 1

Station 20

Apparent Velocities and Intercept Times

Layer No	Velocity (km/sec)		Intercept Time (sec)	
	S.W	N.E	S.W	N.E
1	1.51	1.51	-	-
2	1.98 ±.01	1.98 ±.01	0.09 ±.01	0.09 ±.01
3	2.70 ±.02	2.70 ±.02	0.40 ±.01	0.40 ±.01
4	3.43 ±.05	3.60 ±.04	0.71 ±.04	0.86 ±.04
5	4.41 ±.02	4.35 ±.02	1.37 ±.01	1.34 ±.01
6	6.32	-	2.14	-

True Velocities, Thicknesses and Dips

Layer No	Velocity (km/sec)	Thickness(km)		Depth(km)		Dip(Deg) relative to surface
		Buoy 2	Buoy 3	Buoy 2	Buoy 3	
1	1.51	0.11	0.11	0.11	0.11	0.0
2	1.98	0.41	0.41	0.52	0.52	0.0
3	2.70	0.82	0.51	1.34	1.03	0.0
4	3.51	1.04	1.67	2.38	2.70	1.70
5	4.38	1.71	1.44	4.09	4.14	-1.74
6	6.31*	-	-	-		-0.26
		4.09	4.14			

* Unreversed velocity from one side of single buoy only.

Author Chetty Parasuraman
Name of thesis Digital Data Processing Of Marine Seismic Records From The South West Indian Ocean. 1974

PUBLISHER:
University of the Witwatersrand, Johannesburg
©2013

LEGAL NOTICES:

Copyright Notice: All materials on the University of the Witwatersrand, Johannesburg Library website are protected by South African copyright law and may not be distributed, transmitted, displayed, or otherwise published in any format, without the prior written permission of the copyright owner.

Disclaimer and Terms of Use: Provided that you maintain all copyright and other notices contained therein, you may download material (one machine readable copy and one print copy per page) for your personal and/or educational non-commercial use only.

The University of the Witwatersrand, Johannesburg, is not responsible for any errors or omissions and excludes any and all liability for any errors in or omissions from the information on the Library website.